Empirical calculation of K-shell fluorescence cross sections for elements in the atomic range $16 \leq Z \leq 92$ by photon effects ranging from 5.46 to 123.6 keV (Three-dimensional formulae).

K. Amari[1,2], A. Kahoul[1,2*], J.M. Sampaio[3,4], Y. Kasri[5,6], J.P. Marques[3,4], F. Parente[7], A. Hamidani[1,2], S. Croft[8], A. Favalli[9,10], S. Daoudi[1,2], B. Deghfel[5], A. Zidi[1,2], B. Berkani[1,2]

[1]*Department of Matter Sciences, Faculty of Sciences and Technology, Mohamed El Bachir El Ibrahimi University, Bordj-Bou-Arreridj 34030, Algeria.*
[2]*Laboratory of Materials Physics, Radiation and Nanostructures (LPMRN), Faculty of Sciences and Technology, Mohamed El Bachir El Ibrahimi University, Bordj-Bou-Arreridj 34030, Algeria.*
[3]*LIP – Laboratório de Instrumentação e Física Experimental de Partículas, Av. Prof. Gama Pinto 2, 1649-003 Lisboa, Portugal.*
[4]*Faculdade de Ciências da Universidade de Lisboa, Campo Grande, C8, 1749-016 Lisboa, Portugal.*
[5]*Department of Physics, Faculty of Sciences, University of Mohamed Boudiaf, 28000 M'sila, Algeria.*
[6]*Theoretical Physics Laboratory, Faculty of Exact Sciences, Bejaia University, 06000 Bejaia, Algeria,*
[7]*Laboratory of Instrumentation, Biomedical Engineering and Radiation Physics (LIBPhys-UNL), Department of Physics, NOVA School of Science and Technology, NOVA University Lisbon, 2829-516 Caparica, Portugal.*
[8]*School of Engineering, Faculty of Science of Technology, Nuclear Science, Engineering Research Group, Lancaster University, Bailrigg, Lancaster, LA1 4YW, United Kingdom.*
[9]*European Commission, Joint Research Centre, Ispra, I-21027, Italy.*
[10]*Los Alamos National Laboratory, P.O. Box 1663, Los Alamos, NM 87545, USA.*
[*]Corresponding author. Tel. /Fax (+213) 035862230.
E-mail address: a.kahoul@univ-bba.dz

Abstract:

The main objective of this study is to obtain three-dimensional empirical K-shell X-ray fluorescence cross-section ($\sigma_{K_\alpha}, \sigma_{K_\beta}$ and $\sigma_{K_{tot}}$) values for a wide range of elements ($16 \leq Z \leq 92$) for photons with energies from 5.46 keV to 123.6 keV, using more than 3300 experimental data values published between 1985 and 2023 by numerous researchers. These data values are fitted using an interpolation method including a three-dimensional function against atomic number Z and excitation energy E, resulting in a three-dimensional plot to estimate empirically a three-dimensional set of K_α, K_β and K_{tot} X-ray fluorescence cross sections. The results of this empirical calculation are compared, for selected elements, with other empirical and experimental values reported in the literature, and a reasonable agreement is observed.

Keywords: K-shell, XRF cross sections, empirical calculation and three-dimensional interpolation.

1. Introduction

Theoretical, experimental, and analytical methods for obtaining K-shell fluorescence cross-section values at various excitation energies, fluorescence yields, vacancy transfer probabilities, and intensity ratios of different elements hold immense significance in both basic and applied research. These fundamental atomic parameters are crucial for several fields, including atomic and molecular physics, radiation physics (transport in matter), dosimetry, space and plasma physics, medical research (such as cancer therapy), agriculture, forensic science, basic nuclear physics, and particularly X-ray fluorescence investigations employing either synchrotron radiation or traditional photon sources [1-4]. K-shell fluorescence cross sections are often the most crucial parameter and play a central role in a variety of applications such as nuclear safeguards and non-destructive assays. To date, only a few studies have attempted to calculate K X-ray fluorescence cross sections (XRFCS) for a wide range of elements. These attempts combined empirical and semi-empirical approaches, including fitting experimental data, in addition to using first-principle theoretical models. Moreover, in the context of X-ray fluorescence applications, two notable tabulations are found in the literature. The first is a theoretical table, compiled by Krause *et al.* [5] giving a comprehensive set of K-XRFCS along with useful formulae and essential parameters for calculating these cross sections. The covered parameters include fluorescence yield, fractional radiation rates, and theoretical partial photoionization cross sections based on Hartree-Slater and Hartree-Fock central potential theories published by Scofield [1]. The second tabulation is that created by Puri *et al.* [6] which is less exhaustive but claims to offer updated data of K-shell $(13 \leq Z \leq 92)$ and L-shell series for $(35 \leq Z \leq 92)$ XRFCS across the incident photon energy range 1-200 keV. Nevertheless, a direct comparison between these two tabulations is generally not possible. Krause's table focuses on individual XRF lines, whereas Puri's tabulation groups lines together. Notably, for

K-shell XRFCS, the values from both tabulations agree well for targets with atomic number $Z > 20$, although they diverge by up to 10% for light elements. Due to limited resolution of experimental d~~ac~~te~~te~~ctors, generally, the K X-rays are grouped as K_α and K_β peaks. In the context K_α and K_β X-ray emissions occur when an atom undergoes electronic transitions. Furthermore, the Seigbahn or International Union of Pure and Applied Chemistry (IUPAC) notations are used to classify radiation transitions [7]. In the Seigbahn notation, the IUPAC $K-L$ transitions are grouped K_α, whereas the IUPAC $K-M$ and $K-N$ transitions are represented by K_β. Notably, K_α is one of the major and the most intense X-ray emission lines that can be seen in X-ray spectra. ~~While other transitions,~~ These fundamental K_α and K_β lines garner much attention due to their importance in various practical applications. For instance, an element can be identified and quantified in a sample using K_α and K_β lines. Also, we notice that K_{tot} is the sum of K_α and K_β transitions. Among researchers who have performed empirical and semi-empirical K-XRFCS calculations, Kup Aylikci *et al.* [8] have deduced experimental and semi-empirical K_α and K_β XRFCS for $_{27}$Co and $_{30}$Zn at 59.5 keV. The experimental and semi-empirical calculations of K_α and K_β XRFCS of $_{24}$Cr and $_{30}$Zn for photon energy of 59.6 keV have been determined by Dogan *et al.* [9]. One year later, Dogan *et al*. [10] established experimental, theoretical, and semi-empirical values of K_α and K_β XRFCS for the same elements, using 59.5 keV gamma-rays. In 2016, the same authors Dogan *et al.* [11] estimated the semi-empirical and experimental K_α and K_β XRFCS of $_{29}$Cu and $_{50}$Sn in pure metals at 59.5 keV. Aylikci *et al*. [12] have determined empirical, semi-empirical, and measured K X-ray fluorescence parameters of some elements in the atomic range $21 \leq Z \leq 30$ excited by 59.5 keV photons. Measured and semi-empirical σ_{K_α} and σ_{K_β} production cross sections of $_{26}$Fe and $_{30}$Zn at 59.5 keV have been published by Kup Aylikci *et al.* [13]. In 2019, the semi-empirical

determination of $K_{\alpha_{1,2}}$, $K_{\beta_{1,3}}$ and $K_{\beta_{2,4}}$ X-ray natural line widths for various elements between $29 \leq Z \leq 74$ at 123.6 keV was performed by Kup Aylikci [14].

The purpose of this work is to obtain empirical K-XRFCS values for a wide range of elements at various excitation energies (5.46 to 123.6 keV). The energy and the atomic number Z ranges were selected due to the availability of experimental data. Over 3300 measured K-shell XRFCS data (1049 for K_{α}, 999 for K_{β} and 1040 for K_{tot}) reported from different sources over the period 1985-2023 from ionization by photon impact were fitted by an analytical function to derive empirical values. Furthermore, these experimental values have been fitted using a three-dimensional function against the atomic number Z and energy E to determine the empirical K-XRFCS data for elements with $16 \leq Z \leq 92$. Finally, the obtained results were summarized in tabular form and compared with other empirical and experimental values.

2. Method of empirical calculation

~~The interaction of radiation with matter is a subject that covers many areas of physics. In most cases, the interaction of photons with matter results in the emission of charged particles (energetic electrons). There are several mechanisms for the interaction of gamma rays with matter, whereas only three principal types have a major role in measuring radiation, namely the photoelectric effect, Compton scattering, and pair production. Other effects, such as photonuclear absorption and Rayleigh scattering, can be ignored because they have a negligible impact on the gamma-ray energy range considered here [15]. It is noteworthy that when photons have low energies (less than 511 keV), gamma rays interact primarily through the photoelectric effect [15,16]. This phenomenon describes the situation in which a photon is absorbed by an atom and an electron is ejected.~~ The interaction of radiation with matter is a subject that covers many areas of physics. In most cases, the interaction of photons with matter results in the emission of charged particles (energetic electrons). There are several mechanisms for the

interaction of gamma rays with matter but the one of interest in the present work is the photoelectric effect [15,16]. This phenomenon describes the situation in which a photon is absorbed by an atom and an electron is ejected. In the energy region above threshold and up to a few hundred keV, dependent on the element, it is the dominant interaction. Once the atom is excited, it will emit Auger electrons or X-rays to return to the ground state [17]. Consequently, the gamma-ray interaction cross-section is a physical quantity that characterizes the probability that photons interact with matter.

The K-shell photoionization cross-section, denoted by $\sigma_{\mathrm{K}}^{\mathrm{I}}$, is mainly influenced by the energy of the incoming photon and the atomic number of the medium it interacts with. In the non-relativistic case (Lorentz factor of the ejected electron ≈ unity), and away from the absorption edge, the K-shell photoionization cross section is given by the following expression [18-21]:

$$\sigma_{\mathrm{K}}^{\mathrm{I}} = CZ^5E^{-7/2} \tag{1}$$

with

$$C = 2^{5/2}\frac{8\pi r_e^2}{3}\alpha^4 \tag{2}$$

where

$\frac{8\pi r_e^2}{3} = \sigma_0$ is the Thomson cross-section, α is the fine structure constant, and r_e is the classical electron radius.

$E = \frac{E_\gamma}{E_e}$ presents the energy of photon in units of electron rest mass energy, where $E_\gamma = h\nu$ is the photon energy given in eV,

$E_e = m_0.c^2$ is the electron rest mass energy in eV, and Z is the atomic number.

Eq. (1) is related to the common unit of barn per atom. Although it is an approximation which neglects the atomic structure of the atom and the ionisation energy, we adopt this equation as a

useful starting point for an analytical representation of the main functional dependence of $\sigma_{\mathrm{K}}^{\mathrm{I}}$ on the physical parameters.

On the other hand, the theoretical K_{ji}- shell XRFCS ($ji = \alpha, \beta$ and tot) are defined as the product of the photoionization cross-section $\sigma_{\mathrm{K}}^{\mathrm{I}}$, the fluorescence yield ω_{K}, and the fractional X-ray emission rate F_{K_i}[22-24]:

$$\sigma_{\mathrm{K}_i} = \sigma_{\mathrm{K}}^{\mathrm{I}} \omega_{\mathrm{K}} F_{\mathrm{K}_i} \qquad (i = \alpha, \beta) \tag{3}$$

$$\sigma_{\mathrm{K}_{tot}} = \sigma_{\mathrm{K}_\alpha} + \sigma_{\mathrm{K}_\beta} = \sigma_{\mathrm{K}}^{\mathrm{I}} \omega_{\mathrm{K}} F_{\mathrm{K}_{\mathrm{tot}}}, \tag{4}$$

where

$$F_{\mathrm{K}_\alpha} = \left(1 + \frac{I_{\mathrm{K}_\beta}}{I_{\mathrm{K}_\alpha}}\right)^{-1}, \quad F_{\mathrm{K}_\beta} = 1 - F_{\mathrm{K}_\alpha} \text{ and } F_{\mathrm{K}_{\mathrm{tot}}} = 1, \tag{5}$$

and $\frac{I_{\mathrm{K}_\beta}}{I_{\mathrm{K}_\alpha}}$ designates the intensity ratio (relative probability) of the K_β and K_α X-ray emissions following the photoionization of the K shell.

In this work, we deduce the empirical $\sigma_{\mathrm{K}_\alpha}$, $\sigma_{\mathrm{K}_\beta}$ and $\sigma_{\mathrm{K}_{\mathrm{tot}}}$ XRFCS, by interpolating the existing experimental cross sections using the three-dimensional ($\sigma_{\mathrm{K}_i}(Z, E)$) analytical function to be described next, although it is emphasized that its graphical representation is three-dimensional.

Based on Eq.s (1), (3), and (4), we deduce that an analytical function for the interpolation of $\sigma_{\mathrm{K}_\alpha}$, $\sigma_{\mathrm{K}_\beta}$ and $\sigma_{\mathrm{K}_{tot}}$ XRFCSs can be expressed in the following form:

$$\sigma_{\mathrm{K}_i} = g(Z, E) \times f(Z) \qquad (i = \alpha, \beta, \text{and tot}), \tag{6}$$

where the K-shell photoionization cross-section $\sigma_{\mathrm{K}}^{\mathrm{I}}$ is fitted by the given equation as:

$$g(Z, E) = cZ^5 E^{-d}. \tag{7}$$

This equation allows the energy dependence to emerge from the data, and we are only using Eq. (1) to motivate the use of a power law energy dependence.

Numerous attempts have been made to represent the fluorescence yield using empirical formulae. Among the authors who utilized empirical calculations, we find Poehn *et al.* [25] who proposed the use of a fourth-degree polynomial, to describe the trend of K-shell fluorescence yield for the elements in the atomic range $12 \leq Z \leq 42$, while Hubbell *et al.* [26] collected more recent measured data and used the polynomial $\sum_{n=0}^{3} a_n Z^n$ as a function of the atomic number Z to estimate the K-shell fluorescence yield. Kahoul *et al.* [27], and Meddouh *et al.* [28] suggested a three-order polynomial to calculate K-shell fluorescence yields.

Motivated by the previously cited works [25-28], our proposed analytic expression for the interpolation of the parameter ω_{K} is described by the following third-degree polynomial:

$$\omega_{\mathrm{K}} = f(Z) = \sum_n a_n Z^n = a_0 + a_1 Z + a_2 Z^2 + a_3 Z^3. \quad (8)$$

Similarly, the product quantities $\omega_{\mathrm{K}} F_{\mathrm{K}_{\alpha,\beta}}$ have been interpolated using Eq. (8). Finally, the analytical function used to deduce the $\sigma_{\mathrm{K}_\alpha}$, $\sigma_{\mathrm{K}_\beta}$ and $\sigma_{\mathrm{K}_{\mathrm{tot}}}$ XRFCS is given as:

$$\sigma_{\mathrm{K}_i} = cZ^5 E^{-d} \times (a_0 + a_1 Z + a_2 Z^2 + a_3 Z^3), \ (i = \alpha, \beta, \text{and tot each with a unit set of a, c, and d}) \quad (9)$$

To establish the fitted parameters of Eq. (9), we used an interpolation method, which is a type of fitting technique. This interpolation process was been carried out with version 5.4 patchlevel 8 of Gnuplots software (an open source plotting utility developed and maintained by a group of volunteers), using in the fit the given interpolation function. Once we had obtained the fitted parameters we plotted the data points and fitting function using the Origin 2021 software (a data analysis and graphing software developed by OriginLab Corporation, Northampton, MA,

USA). The specific Gnuplot scripts used for this technique are provided in the Appendix section.

The deviation of the experimental data ($\sigma_{K_i-\mathrm{exp}}$) from their associated fitted values ($\sigma_{K_i-\mathrm{emp}}$) is quantified using the root-mean-square errors $\varepsilon_{\mathrm{rms}}(\%)$ as follows:

$$\varepsilon_{\mathrm{rms}} = \left[\sum_{i=1}^{N} \frac{1}{N}\left(\frac{\sigma_{K_i-\mathrm{exp}}-\sigma_{K_i-\mathrm{emp}}}{\sigma_{K_i-\mathrm{emp}}}\right)^2\right]^{1/2}, \quad (10)$$

where N is the number of data points. The root-mean-square error ($\varepsilon_{\mathrm{rms}}$) is frequently used to express the overall quality of the empirical fits to data.

3. Results and discussion

The database used in this study to calculate the empirical K_α, K_β and K_{tot} XRFCS for targets with atomic number $16 \leq Z \leq 92$ for photon energy ranging from 5.46 to 123.6 keV relies mainly on the experimental data compilations published recently by our group [29]. To generate empirical σ_{K_α}, σ_{K_β} and $\sigma_{K_{\mathrm{tot}}}$ XRFCS that are dependable and consistent, enhance the quality of the interpolation, and produce a satisfactory fitting, we divided the range of excitation energy into two ranges: the first is from 5.46-60 keV and the second is from 60 to123.6 keV. It should be pointed out that some of the experimental values from the used database were not included in the fitting process, such as the experimental data of Uğurlu and Demir [23], for $_{25}$Mn without magnetic field at 59.54 keV, some elements published by Durak *et al*. [30] ($_{23}$V, $_{27}$Co, $_{30}$Zn, and $_{34}$Se), and those reported by Yashoda *et al.* [31] and therefore do not influence the interpolation.

It is crucial that the number of free model parameters must be less than the number of points and moreover the dynamic range must be adequate to define the shape of data. For instance, it would be pointless to try and fit a third order polynomial in Z to 100 data points if all the points

were for Z=47. It is the number of Z 'clusters' that must exceed the number of free parameters. That is why we have used low order polynomials so as to avoid spurious shapes that are a consequence of over-fitting.

For each Z, a statistical analysis can estimate a single 'best value' to be used in the fit. But the fitting procedure effectively carries out this 'weighting' for you. The fit emphasizes where the data is most concentrated and reliable. Although we must appreciate that the fits are empirical and not based on a highly detailed underlying physical model, but with this in mind the fits are robust and reliability is reasonably assessed by the deviations observed.

Regarding the nature of the fitted data, there may be multiple values at a given E for a given Z and as noted above one could choose to collapse that data to a single point prior to fitting. In contrast, the mathematical principles behind the fitting process perform that smoothing or averaging for you automatically.

Furthermore, we plotted the experimental K_α, K_β and K_{tot} XRFCS against atomic number and energy *E*, and then fitted the points using Eq. (6). The fitting results are displayed in Fig.s 1-6, whereas the fitting coefficients for Eq.s (7) and (8) are listed in Table 1. It is crucial to highlight that the fitting equation (6) and its associated coefficients are only applicable within the range of the used experimental data. Additionally, any extension of the fittings outside the corresponding ranges might lead to erroneous cross-section values. Moreover, we noticed that a portion of the experimental data scatter can be attributed to the fact that the data were acquired from a variety of references and sources and measured under different conditions.

To illustrate the deviation of the various empirical results graphically, a comparison was made between our empirical values of K_α, K_β and K_{tot} XRFCS and empirical results created by Puri *et al.* [6] and other experimental findings as a function of the photon energy for selected elements, namely $_{28}$Ni, $_{42}$Mo and $_{57}$La, the selection of these elements being due to the extensive

experimental dataset available. The results of this comparison for $\sigma_{K_\alpha}, \sigma_{K_\beta}$ and $\sigma_{K_{tot}}$ XRFCS are shown in Fig.s 7-9, respectively. Additionally, to check our calculations, a compar~~a~~ison of current empirical K_α, K_β and K_{tot} XRF cross-sections with the experimental works of [32-38] is presented in Tables 2-4, respectively. Besides, ~~T~~the graphical representation in the Fig.s 7-9 employs a specific symbol to distinguish between our empirical results (K_α, K_β and K_{tot} XRFCS), the empirical values documented in the Puri *et al.* [6] research, and experimental measurements, allowing for a detailed comparison of the different sets of data. The examination of these figures allows for some comments:

Our analysis reveals good general agreement between our empirical $\sigma_{K_\alpha}, \sigma_{K_\beta}$ and $\sigma_{K_{tot}}$ XRFCSs data and those reported by Puri *et al.* [6] across the energy range from 8 to 60 keV for $_{28}$Ni. Subsequently, within the specified 20-150 keV energy range, there is a strong concordance between our empirical findings estimated using Eq. (6) for $_{42}$Mo and those of Puri *et al.* [6]. Also, the obtained empirical values of K_α, K_β and K_{tot} XRFCS for $_{57}$La coincide quite well with Puri's values published for the photon's energy ranging from 40 to 80 keV. Furthermore, Fig.s 7-9 depict notable agreement among our empirical $\sigma_{K_\alpha}, \sigma_{K_\beta}$ and $\sigma_{K_{tot}}$ XRFCS and experimental values of [32-34] over a whole range of energy used for $_{28}$Ni, whereas, for the same element $_{28}$Ni, it can be said that for some excitation-energy values, the agreement between our empirical calculation and those experimental values are not satisfying. Besides, the empirical results align closely with the experimental values of Demir and Şahin [35] for the targets $_{28}$Ni and $_{57}$La at an excitation energy of 59.5 keV. Moreover, for $_{42}$Mo and $_{57}$La, we notice an excellent agreement between the empirical values for $\sigma_{K_\alpha}, \sigma_{K_\beta}$ and $\sigma_{K_{tot}}$ XRFCS and the values established by Seven and Erdoğan [36] across energy range from 50 to 80 keV. In addition, the comparison reveals a quite good agreement between our empirical and those obtained experimentally [34,37] for $_{42}$Mo in multiple excitation energies ranging from 21 to

51 keV. Also, our empirical values for $\sigma_{K_\alpha}, \sigma_{K_\beta}$ and $\sigma_{K_{tot}}$ XRFCS exhibit a satisfactory agreement with the experimental data of Özdemir *et al.* [38] for $_{42}$Mo at 59.5 keV. Furthermore, the examination of Fig. 7 requires additional comments:

In general, for σ_{K_α}, the deviations between our current calculation and the experimental data of Baydaş *et al.* [32] for $_{28}$Ni vary in the range 0.35%-16.53%, and from 0.94% to 9.14% relative to Rao *et al*. [34]. A notable variation is observed for the measured values of Singh *et al.* [33] and Demir and Şahin [35] with deviations of 135.71%, 30.48%, 92.85%, 29.94%, and 22,94% for $_{28}$Ni. In addition, for $_{42}$Mo the deviations between the present empirical results and the other experimental values are about: 0.6%-8.82% for Seven [37] 0.80%-3.82% for Demir and Şahin [35], 2.87%-9.37% for Seven and Erdoğan [36], and 11.21%-12.12% for the values of Özdemir *et al.* [38]. For $_{57}$La, our calculation agrees within 1.17%-8.18% and 2.31%-2.57% with the measured values of Seven and Erdoğan [36], and Demir and Şahin [35], respectively.

From Fig. 8, it can be seen that for $_{28}$Ni our empirical values exhibit a good agreement, with deviations varying from 6.12% to 18.25%, except for the considering photon energy with deviations of 25.02% for Baydaş *et al.* [32], 0.85%-10.02% for Singh *et al.* [33], and 1.03% to 16.05% for Rao *et al.* [34], notably for the energy values of 11.4 keV, 22.6 keV, and 46.9 keV, the deviations are 36.09%, 22.73%, and 27.75%, respectively. For $_{42}$Mo, the deviations vary from 0.71% to 10.85% for Seven [37], 8.88%-14.74% for Rao *et al*. [34], 5.80%-13.52% for Seven and Erdoğan [36], and 5.41%-10.52% for Özdemir *et al.* [38]. Finally, for $_{57}$La, the deviations between the present empirical values and the values from other authors are about 2.96%-13.52% for Seven and Erdoğan [36], and 2.69%-6.64% for Demir and Şahin [35].

It is conspicuous from Fig. 9 that for $_{28}$Ni the observed deviations vary from 0.01% to 13.71% for Baydaş *et al.* [32], 2.09%-10.94% for Singh *et al.* [33], except for excitation-energy values 41 keV and 46.9 keV with deviations of 21.2% and 29.03%, 8.86%-17.75% for Rao *et al.* [34],

and with deviations of 18.95% for Demir and Şahin [35], except for energy of 59.5 keV without magnetic field with a deviation of 28.91%. Moreover, for $_{42}$Mo we observed that the agreement between the data is very good and the deviations are about: 0.90%-5.61% using the values of Seven [37], 0.31%-3.69% for Rao *et al.* [34], 2.54%-10.16% for the data of Seven and Erdoğan [36], and 11.98%-13.26% for Özdemir *et al.* [38]. Finally, for $_{57}$La the deviation ranged from 0.51% to 9.59% for Seven and Erdoğan [36], and between 0.26% and 5.41% for Demir and Şahin [35]. We notice that the formula used to calculate the deviations between our empirical values and other experimental values is

$$D(\%) = \left|\frac{\sigma_{\mathrm{K}_i} - \sigma_{\mathrm{K}_i\mathrm{-emp}}}{\sigma_{\mathrm{K}_i\mathrm{-emp}}}\right| \times 100 \text{ for} \qquad (11)$$

4. Conclusion

The K shell X-ray fluorescence cross-section measurements reported in the literature covering the period from 1985 to 2023 (about 3300 experimental data) were used to deduce new empirical values for the $\mathrm{K}_\alpha, \mathrm{K}_\beta$ and $\mathrm{K}_{\mathrm{tot}}$ XRFCS with their corresponding fitting parameters using a three-dimensional interpolation for elements in the atomic region $16 \leq Z \leq 92$ for photon energies ranging from 5.46 to 123.6 keV. All over the atomic number range, the predicted empirical $\sigma_{\mathrm{K}_\alpha}, \sigma_{\mathrm{K}_\beta}$, and $\sigma_{\mathrm{K}_{\mathrm{tot}}}$ XRFCS were notably closer to experimental data. Furthermore, our empirical results for the elements $_{28}$Ni, $_{42}$Mo and $_{57}$La were compared with experimental and other empirical values. Our findings exhibit a satisfactory agreement with previously published data (experimental and Puri's empirical data) over the whole photon energy range.

Acknowledgments

We gratefully acknowledge the support of the DGRSDT, Ministry of Higher Education and Scientific Research, Algeria. This work was done with the support of Mohamed El Bachir El

Ibrahimi University, under project (PRFU) N°: B00L02UN340120230003. This work was also supported by the Fundação para a Ciência e Tecnologia (FCT), Portugal through contracts UIDP/50007/2020 (LIP) and UID/FIS/04559/2020 (LIBPhys). S.C. warmly acknowledges the financial support of Lancaster University, and A.F. gratefully acknowledges the support of the Joint Research Centre of the European Commission.

Figures captions

Fig. 1. The distribution of the experimental K_{α} XRFCS as a function of atomic number *Z* and photon energy range of 10-60 keV. The interpolation result is also presented as a surface.

Fig. 2. The distribution of the experimental K_{α} XRFCS as a function of atomic number *Z* and photon energy range of 60-130 keV. The interpolation result is also presented as a surface.

Fig. 3. The distribution of the experimental K_{β} XRFCS as a function of atomic number *Z* and photon energy range of 10-60 keV. The interpolation result is also presented as a surface.

Fig. 4. The distribution of the experimental K_{β} XRFCS as a function of atomic number *Z* and photon energy range of 60-130 keV. The interpolation result is also presented as a surface.

Fig. 5. The distribution of the experimental K_{tot} XRFCS as a function of atomic number *Z* and photon energy range of 10-60 keV. The interpolation result is also presented as a surface.

Fig. 6. The distribution of the experimental K_{tot} XRFCS as a function of atomic number *Z* and photon energy range of 60-130 keV. The interpolation result is also presented as a surface.

Fig. 7. A comparison between empirical K_α XRFCS results determined using Eq. (6), the ~~empirical~~ values of Puri *et al.* [6], and the experimental findings as a function of the photon energy for $_{28}$Ni, $_{42}$Mo and $_{57}$La.

Fig. 8. A comparison between empirical K_β XRFCS results determined using Eq. (6), the ~~empirical~~ values of Puri *et al*. [6], and the experimental findings as a function of the photon energy for $_{28}$Ni, $_{42}$Mo and $_{57}$La.

Fig. 9. A comparison between empirical K_{tot} XRFCS results determined using Eq. (6), the ~~empirical~~ values of Puri *et al*. [6], and the experimental findings as a function of the photon energy for $_{28}$Ni, $_{42}$Mo and $_{57}$La.

Appendix

#Reset in Gnuplot is to clear any previous settings

gnuplot> reset

#Load your data file par example as “file.dat”

gnuplot> load “file.dat”

#To plot the data we use “splot” for 3D plots

gnuplot> splot”file.dat”

#Label and titel

gnuplot> set xlabel “Z”

gnuplot> set ylabel “E”

gnuplot> set zlabel “Exp”

gnuplot> set titel“3D plot”

#Define the fitting function”f(x,y)”

gnuplot> f(x,y) =(c*x**5)*(y**(-d))*(a_0+a_1*x+a_2*x*x+a_3*x*x*x)

#We use the ‘fit’ command to fit the function f(x,y) to the data points using columns 1,2,3 for ‘x’,’y’ and ‘z’ values respectively, and obtained the fitted parameters after several iterations.

gnuplot> fit f(x,y) “file.dat” using 1:2:3 via c,d, a_0, a_1, a_2, a_3

References:

[1] Scofield, J. H., California Univ., Livermore. Lawrence Livermore Lab. No. UCRL-51326 (1973).

[2] Hubbell, J. H. and Seltzer, S. M., National Institute of Standards and Technology, Gaithersburg, MD. No NIST IR 5632 (1995).

[3] Berger, M. J., Hubbell, J. H., Seltzer, S. M. and Chang, J., J. Appl. Phys. 58(10) 2333-2342 (2010).

[4] Hakcley, M. S., Springer Science and Business Media. (2011).

[5] Krause, M. O., Nestor, C. W. Jr., Sparks, C. J. Jr. and Ricci, E., Oak. Ridge. National. Lab. No. ORNL-5399, 7032250 (1978).

[6] Puri, S., Chand, B., Mehta, D., Garg, M. L., Singh, N. and Trehan, P. N., At. Data Nucl. Data Tables. 61, 289–311 (1995).

[7] Jenkins, R., Manne, R., Robin, R. and Senemaud, C., Pure Appl. Chem. 63(5), 735-746. (1991).

[8] Kup Aylikci, N., Aylikci, V., Kahoul, A., Tiraşoğlu, E., Karahan, İ. H. and Cengiz, E., Phys. Rev. A. 84 042509 (2011).

[9] Dogan, M., Tirasoglu, E., Karahan, İ. H., Kup Aylikci, N., Aylikci, V., Kahoul, A., Cetinkara, H. A. and Serifoglu, O., Radiat. Phys. Chem. 87, 6–15 (2013).

[10] Dogan, M., Aylikci, V., Tiraşoglu, E. and Karahan, İ. H., J. Radiat. Res. Appl. Sci. 7, 241–248 (2014).

[11] Dogan, M., Olgar, M. A., Cengiz, E. and Tıraşoglu, E., Radiat. Phys. Chem. 126, 111–115 (2016).

[12] Aylikci, V., Kahoul, A., Aylikci, N. K., Tiraşoğlu, E. and Karahan, İ. H., Spectrosc. Lett. 48, 331–342 (2015).

[13] Kup Aylikci, N., Sampaio, J. M., Kahoul, A., Aylikci, V., Karahan, I. H., Guerra, M., Santos, J. P., Marques, J. P. and Tiraşoğlu, E., X-Ray Spectrom. 46, 242–251 (2017).

[14] Kup Aylikci, N., Spectrosc. Lett. 52, 346–355 (2019).

[15] Knoll, G. F., Radiation Detection and Measurement (4th Edition). Wiley (2010).

[16] Zettili, N., Quantum mechanics: concepts and applications, 2nd ed. Wiley, Chichester, U.K (2009).

[17] Storm, L. and Israel, H. I., At. Data Nucl. Data Tables. 7(6), 565-681 (1970).

[18] Ranganathaiah, C., Umesh, T. K. and Sanjeevaiah, B., Nucl. Scie. Engin. 90, 99–102 (1985).

[19] Heitler, W., In the Quantum Theory of Radiation 3rd edn, p. 204. Oxford University Press, London. (1954).

[20] Davisson, C. M., Interaction of γ- radiation with matter. See also App. 1 at the end of this volume., in: Alpha-, Beta- and Gamma-Ray Spectroscopy. Elsevier, pp. 37–78 (1968).

[21] Legarda, F., Herranz, M. and Lafuente, O. M. D., Int. J. Radiat Appl. Instrum. Part A. Appl. Radiat. Isot. 40, 85–88 (1989).

[22] Sirin, M., Baltas, H., Kiris, E. and Keskenler, E. F., Spectrosc. Lett. 52, 98–104 (2019).

[23] Uğurlu, M. and Demir, L., Spectrosc. Lett. 53, 163–171 (2020).

[24] Turhan, M. F. and Akman, F., Nucl. Instrum. Methods Phys. Res. Sect. B Beam Interact. Mater. At. 534, 16–25 (2023).

[25] Poehn, C., Wernisch, C. and Hanke, W., X-Ray Spectrom. 14, 120-124 (1985).

[26] Hubbell, J. H., Trehan, P. N., Singh, N., Chand, B., Mehta, D., Garg, M. L., Garg, R. R., Singh, S. and Puri, S., J. Phys. Chem. Ref. Data. 23, 339–364 (1994).

[27] Kahoul, A., Aylikci, V., Aylikci, N. K., Cengiz, E. and Apaydın, G., Radiat. Phys. Chem .81, 713–727 (2012).

[28] Meddouh, K., Daoudi, S., Kahoul, A., Sampaio, J. M., Marques, J. P., Parente, F., Aylikci, N. K., Aylikci, V., Kasri, Y. and Hamidani, A., Radiat. Phys. Chem. 202, 110481 (2023).

[29] Amari, K., Kahoul, A., Sampaio, J. M., Daoudi, S., Marques, J. P., Parente, F., Hamidani, A., Croft, S., Favalli, A., Kasri, Y., Zidi, A. and Berkani, B., At. Data Nucl. Data Tables in press (2024).

[30] Durak, R., Ateş, A., Turhan, M. F. and Sağlam, M., In Proceedings of the International Conference Nanomaterials: Applications and Properties (No. 1, no. 4, pp. 04RES10-04RES10). Sumy State University Publishing (2012).

[31] Yashoda, T., Krishnaveni, S., Gowda, S., Umesh, T. and Gowda, R., Pramana. 58, 31–38 (2002).

[32] Baydaş, E., Şahin, Y. and Büyükkasap, E., J. Trace Microprobe Tech. 21, 433–442 (2003).

[33] Singh, S., Rani, R., Mehta, D., Singh, N., Mangal, P. C. and Trehan, P. N., X-Ray Spectrom. 19, 155–158 (1990).

[34] Rao, D. V., Cesareo, R. and Gigante, G. E., Appl. Phys. Solids Surf. 56, 401–403 (1993).

[35] Demir, D. and Şahin, Y., Radiat. Phys. Chem. 85, 64–69 (2013).

[36] Seven, S. and Erdoğan, H., Radiat. Phys. Chem. 117, 1–6 (2015).

[37] Seven, S., Radiat. Phys. Chem. 81, 489–494 (2012).

[38] Özdemir, Y., Kavaz, E., Ahmadi, N., Ertuğrul, M. and Ekinci, N., Appl. Radiat. Isot. 115, 147–154 (2016).

Fig. 1

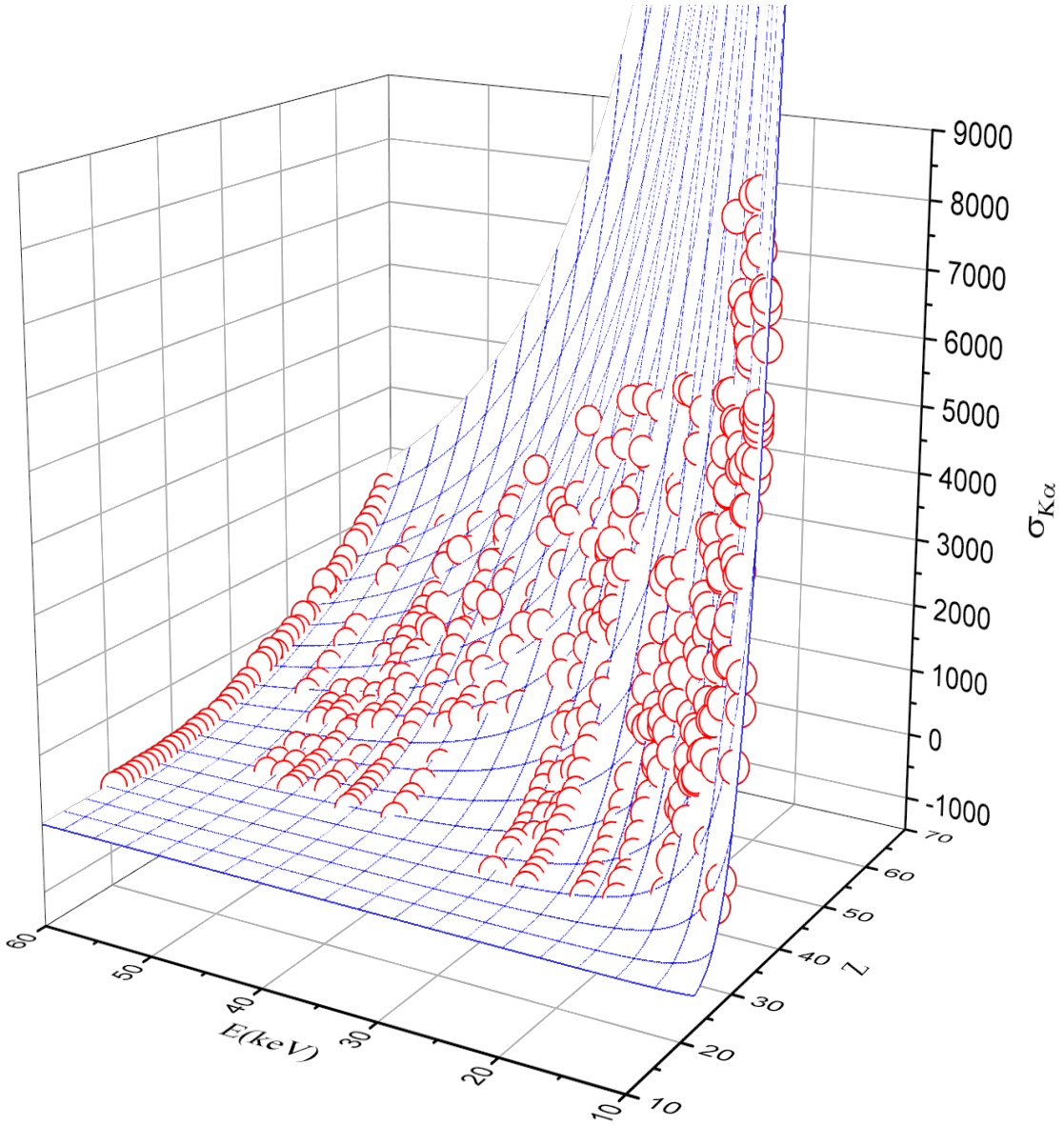
9000
8000
7000
6000
5000
4000
3000
2000
1000
0
-1000
$\sigma_{K\alpha}$
60
50
40
30
20
10
E(keV)
70
60
50
40
30
20
10
Z

Fig. 2

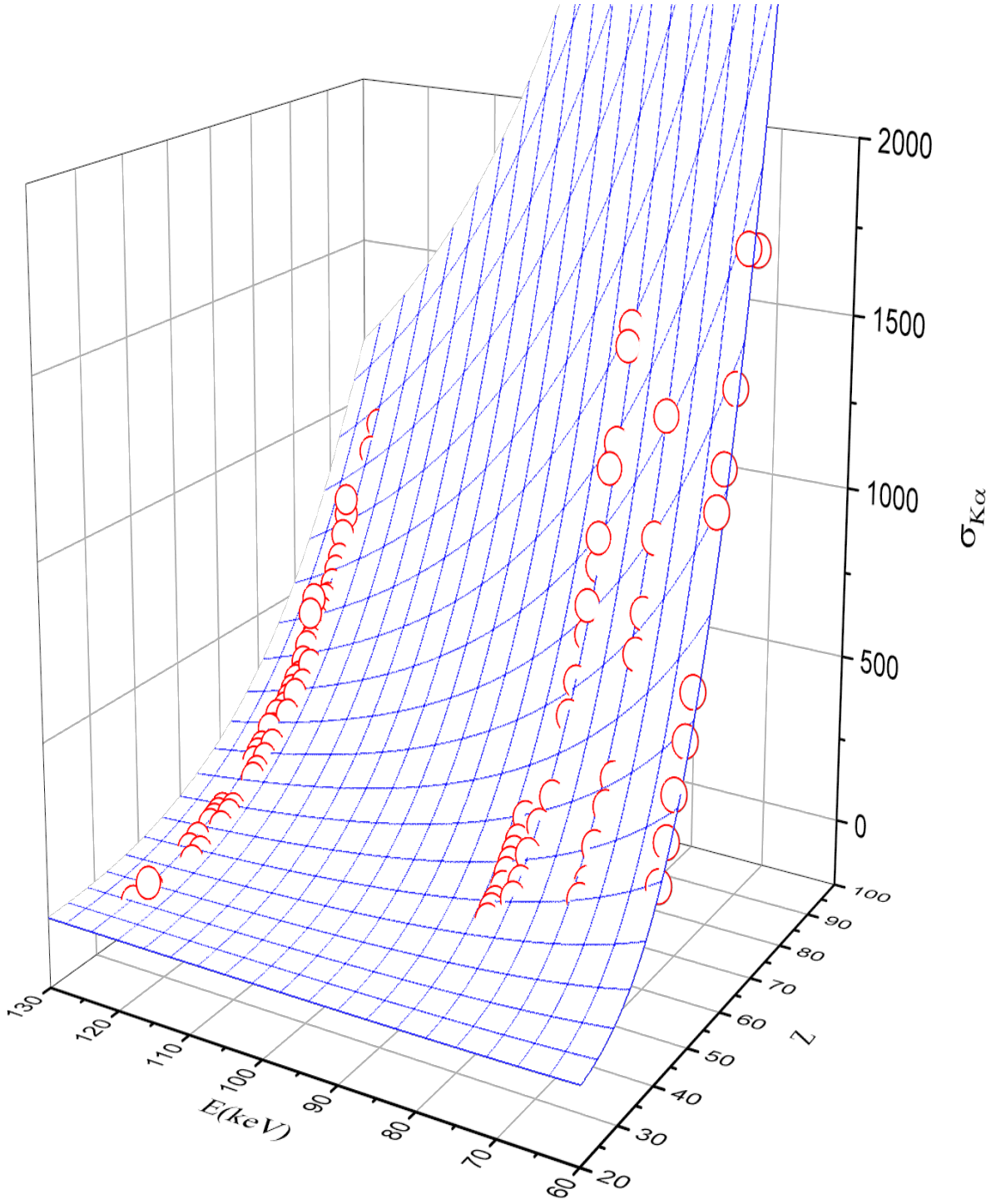
2000
1500
1000
500
0
$\sigma_{K\alpha}$
130
120
110
100
90
80
70
60
E(keV)
100
90
80
70
60
50
40
30
20
Z

Fig. 3

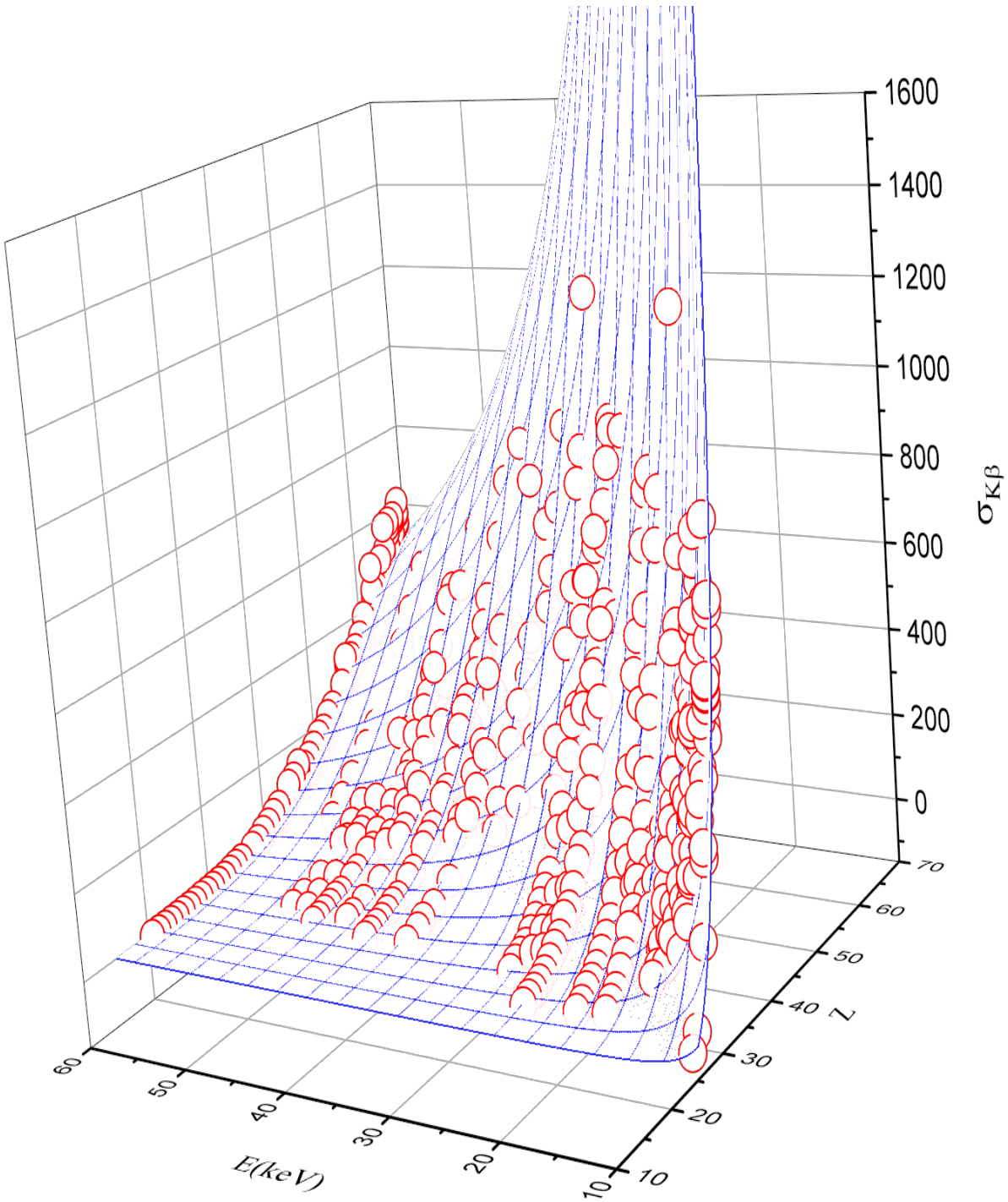
1600
1400
1200
1000
800
600
400
200
0
$\sigma_{K\beta}$
70
60
50
40
Z
30
20
10
60
50
40
30
20
10
E(keV)

Fig. 4

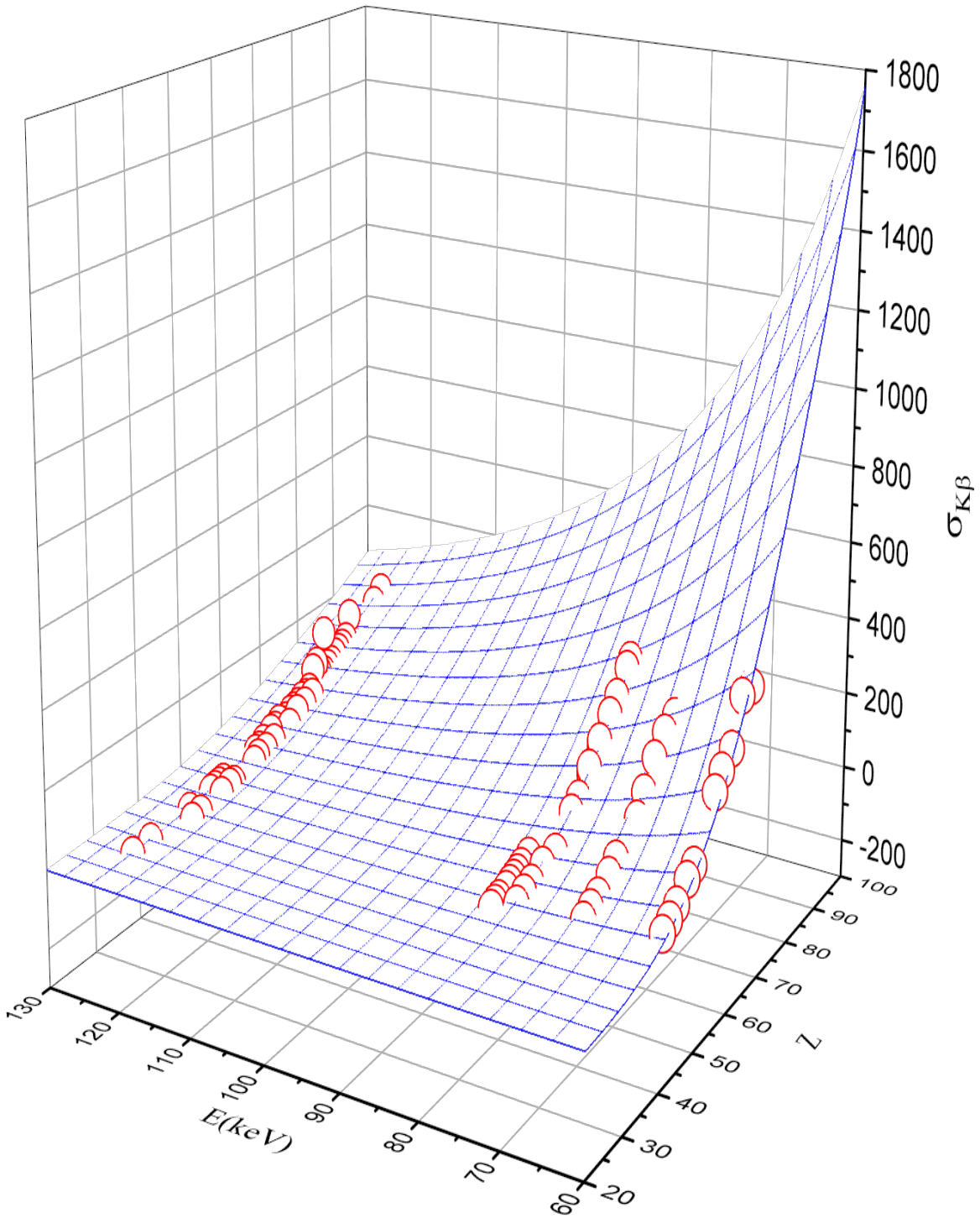
1800
1600
1400
1200
1000
800
600
400
200
0
-200
$\sigma_{K\beta}$
130
120
110
100
90
80
70
60
E(keV)
100
90
80
70
60
50
40
30
20
Z

Fig. 5

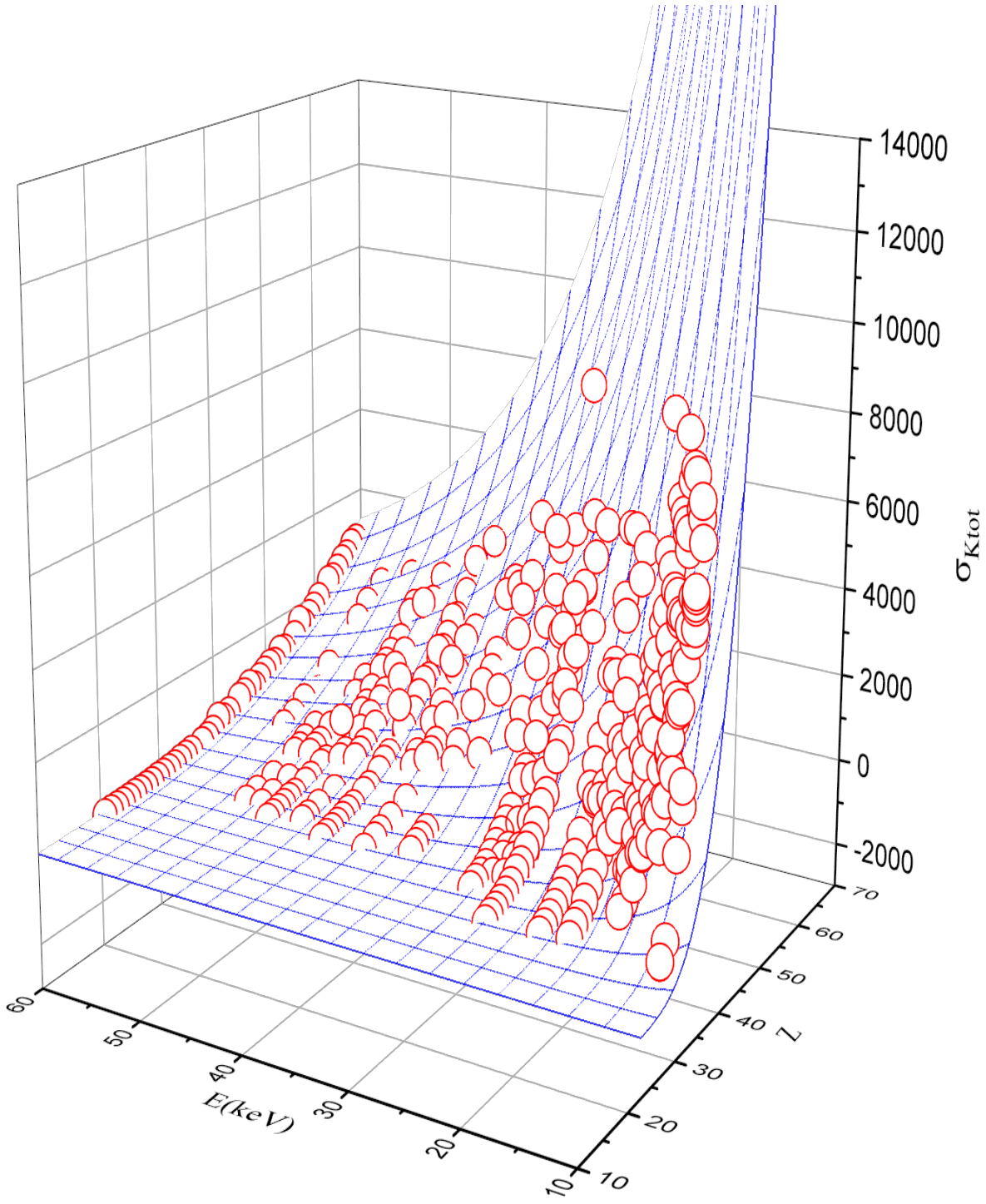
14000
12000
10000
8000
6000
4000
2000
0
-2000
σKtot
60
50
40
30
20
10
E(keV)
70
60
50
40
30
20
10
Z

Fig. 6

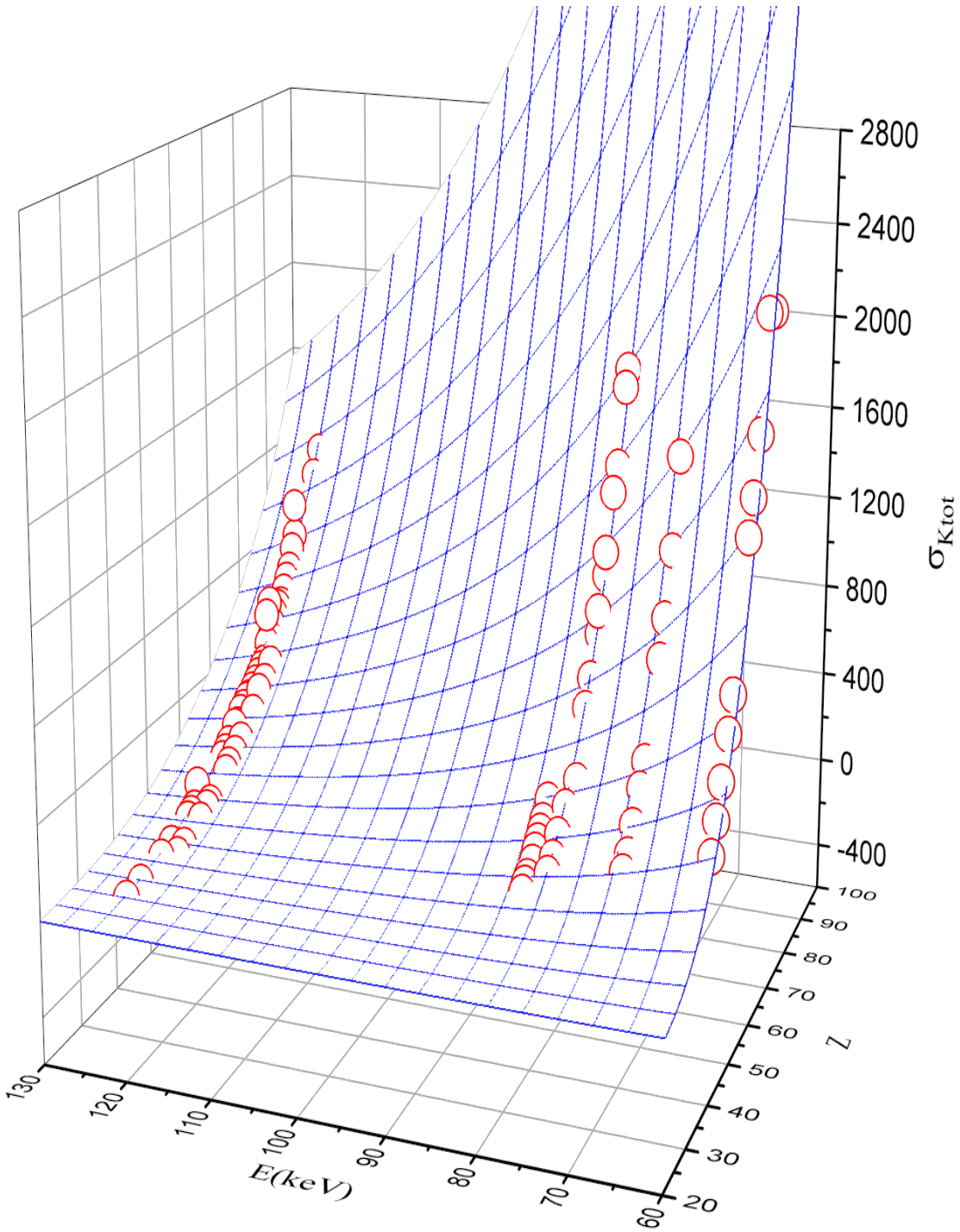
2800
2400
2000
1600
1200
800
400
0
-400
σKtot
100
90
80
70
60
50
40
30
20
Z
130
120
110
100
90
80
70
60
E(keV)

Fig. 7

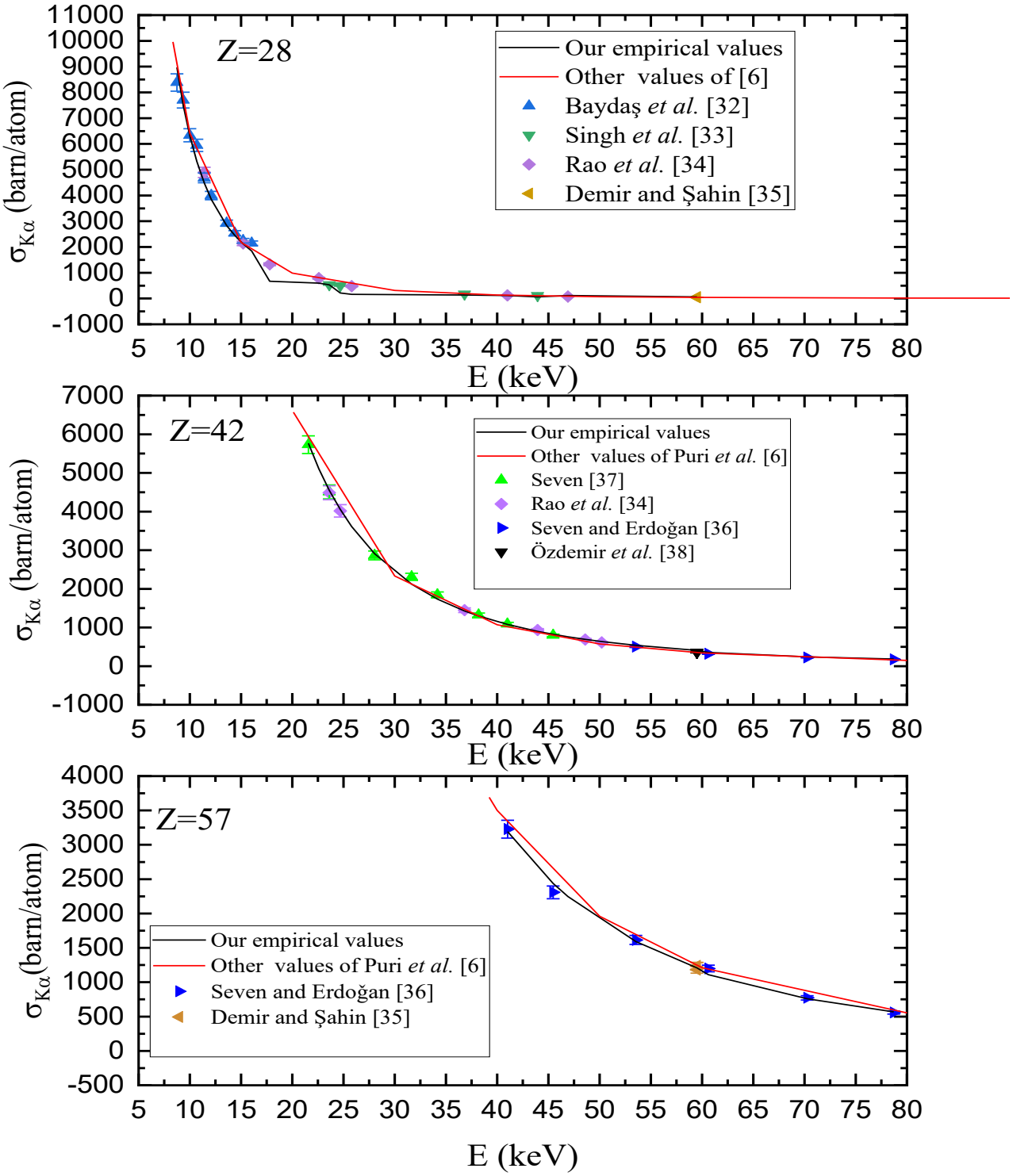
Z=28
Our empirical values
Other values of [6]
Baydaş et al. [32]
Singh et al. [33]
Rao et al. [34]
Demir and Şahin [35]
σKα (barn/atom)
E (keV)
Z=42
Our empirical values
Other values of Puri et al. [6]
Seven [37]
Rao et al. [34]
Seven and Erdoğan [36]
Özdemir et al. [38]
σKα (barn/atom)
E (keV)
Z=57
Our empirical values
Other values of Puri et al. [6]
Seven and Erdoğan [36]
Demir and Şahin [35]
σKα (barn/atom)
E (keV)

Fig. 8

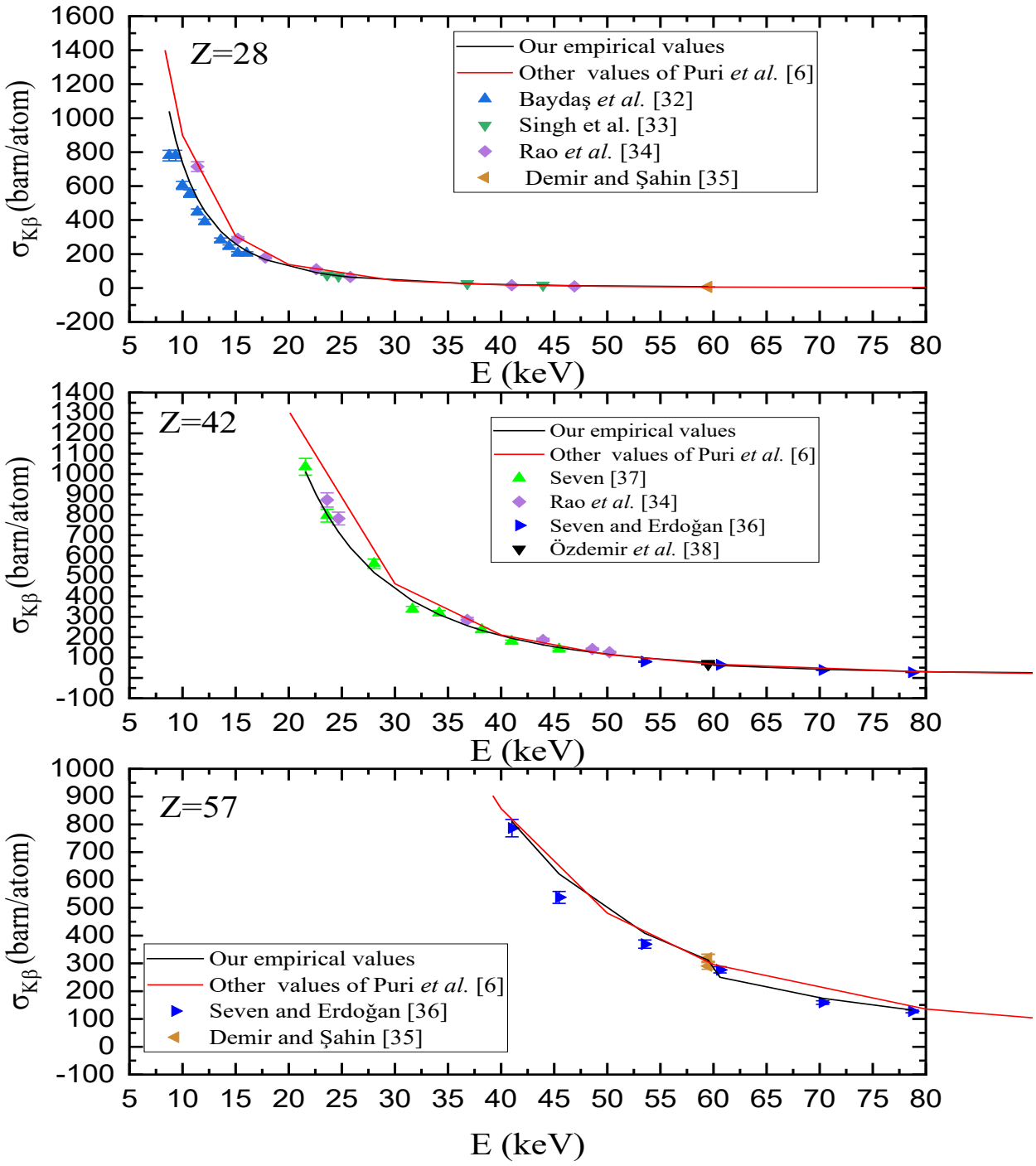
Z=28
Our empirical values
Other values of Puri et al. [6]
Baydaş et al. [32]
Singh et al. [33]
Rao et al. [34]
Demir and Şahin [35]
σKβ (barn/atom)
E (keV)
Z=42
Our empirical values
Other values of Puri et al. [6]
Seven [37]
Rao et al. [34]
Seven and Erdoğan [36]
Özdemir et al. [38]
σKβ (barn/atom)
E (keV)
Z=57
Our empirical values
Other values of Puri et al. [6]
Seven and Erdoğan [36]
Demir and Şahin [35]
σKβ (barn/atom)
E (keV)

Fig. 9

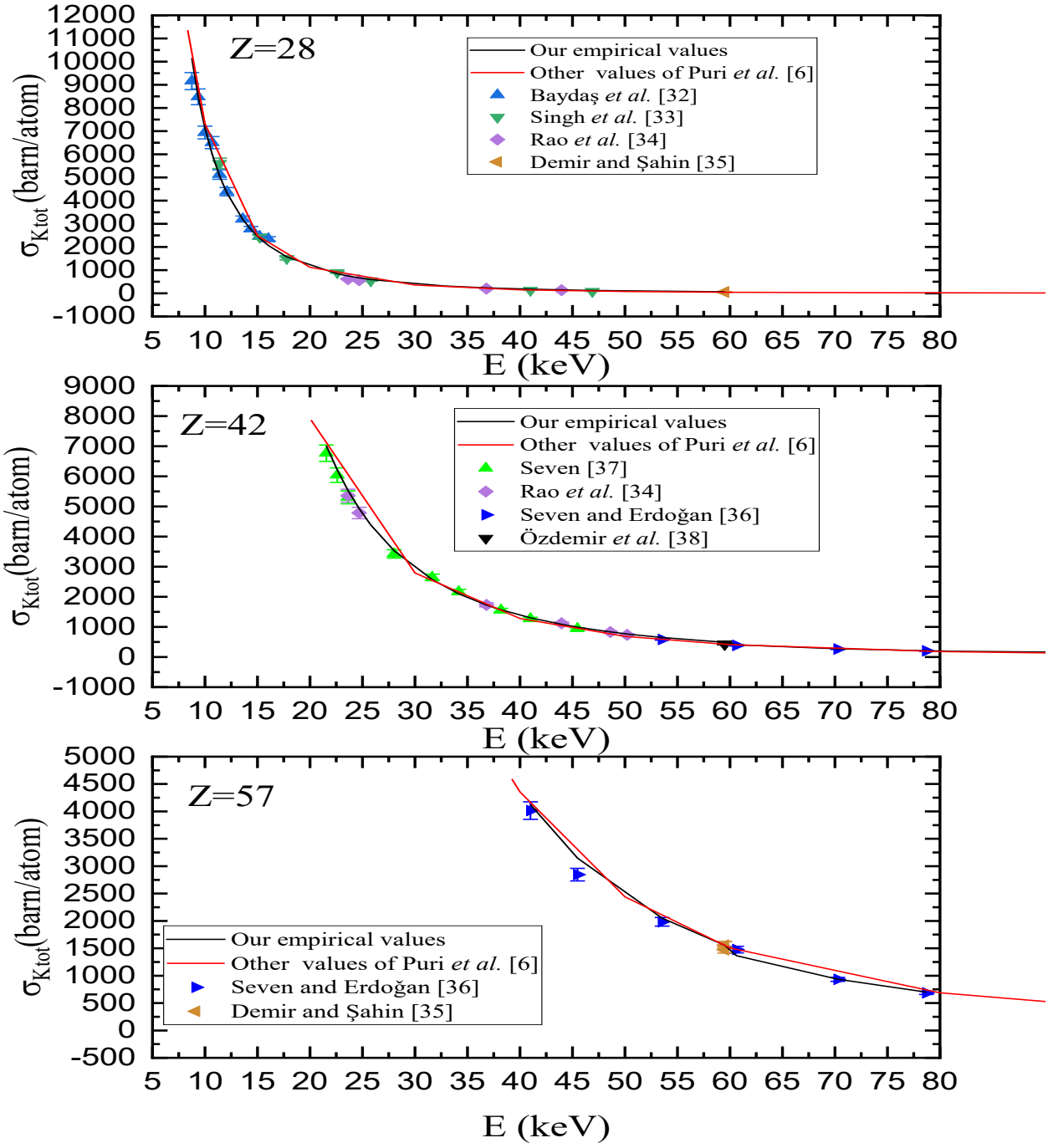
Z=28
Our empirical values
Other values of Puri et al. [6]
Baydaş et al. [32]
Singh et al. [33]
Rao et al. [34]
Demir and Şahin [35]
σKtot (barn/atom)
E (keV)
Z=42
Our empirical values
Other values of Puri et al. [6]
Seven [37]
Rao et al. [34]
Seven and Erdoğan [36]
Özdemir et al. [38]
σKtot (barn/atom)
E (keV)
Z=57
Our empirical values
Other values of Puri et al. [6]
Seven and Erdoğan [36]
Demir and Şahin [35]
σKtot (barn/atom)
E (keV)

Table 1. The fitting coefficients for the calculation of the empirical K_α, K_β and K_{tot} XRF cross section for photon energy range according to the formulae (7) and (8). The associated root-mean-square errors (ε_{rms}) are also included.

	Z-range	E-range (keV)		a_i, c, d	Values	ε_{rms}(%)
σ_{K_α}	$16 \le Z \le 68$	$5.46 \le E \le 60$	$f(Z)$	a_0	-365772	17.14
				a_1	58052.5	
				a_2	-1366.86	
				a_3	9.30433	
			$g(Z,E)$	c	3.80364×10^{-7}	
				d	2.6094	
	$29 \le Z \le 92$	$60 \le E \le 123.6$	$f(Z)$	a_0	2.11224×10^{6}	29.57
				a_1	-50706.2	
				a_2	484.629	
				a_3	-1.66603	
			$g(Z,E)$	c	1.40195×10^{-7}	
				d	2.56346	
σ_{K_β}	$16 \le Z \le 68$	$5.46 \le E \le 60$	$f(Z)$	a_0	-902971	17.14
				a_1	99092.7	
				a_2	-1178.39	
				a_3	1.30357	
			$g(Z,E)$	c	1.63094×10^{-8}	
				d	2.57106	
	$29 \le Z \le 92$	$60 \le E \le 123.6$	$f(Z)$	a_0	126244	14.13
				a_1	185799	
				a_2	-3184.16	
				a_3	14.4306	
			$g(Z,E)$	c	3.12827×10^{-9}	
				d	2.44575	
$\sigma_{K_{tot}}$	$16 \le Z \le 68$	$5.46 \le E \le 60$	$f(Z)$	a_0	-355738	19.67
				a_1	48200.6	
				a_2	-1058.88	
				a_3	6.79281	
			$g(Z,E)$	c	5.54307×10^{-7}	
				d	2.62177	
	$29 \le Z \le 92$	$60 \le E \le 123.6$	$f(Z)$	a_0	1.77959×10^{6}	12.16
				a_1	-24359.9	
				a_2	57.0965	
				a_3	0.400256	
			$g(Z,E)$	c	1.2421×10^{-7}	
				d	2.55326	

Table 2. Comparaison of empirical K_α X-ray fluorescence cross-section (in barn) deduced from this work by photon impact with the experimental values of [32-38].

E(KeV)	**Our results**	**Other Experimenrales works**						
	Empirical values	Baydaş *et al.* [32]	Rao *et al*. [34]	Singh *et al.* [33]	Demir and Şahin [35]	Seven [37]	Seven and Erdoğan [36]	Özdemir *et al.* [38]
$_{28}$Ni								
8.74	8971.38	8382	--	--	--	--	--	--
9.36	7502.26	7699	--	--	--	--	--	--
10	6313.05	6335	--	--	--	--	--	--
10.68	5317.23	5945	--	--	--	--	--	--
11.4	4484.89	4678	4895	--	--	--	--	--
12.09	3847.3	3996	--	--	--	--	--	--
13.6	2829.98	2924	--	--	--	--	--	--
14.38	2446.71	2534	--	--	--	--	--	--
15.2	2117.08	2242	2137	--	--	--	--	--
16.04	1839.84	2144	--	--	--	--	--	--
17.8	670.2	--	1327	--	--	--	--	--
22.6	597.66	--	787	--	--	--	--	--
23.62	532.3	--	--	538	--	--	--	--
24.68	210.43	--	--	496	--	--	--	--
25.8	158.94	--	475	--	--	--	--	--
36.82	132.59	--	--	173	--	--	--	--
41	111.91	--	122	--	--	--	--	--
43.95	60.15	--	--	116	--	--	--	--
46.9	111.91	--	78	--	--	--	--	--
59.5	60.15	--	--	--	46.35	--	--	--
$_{42}$Mo								
21.57	5764.32	--	--	--	--	5730.02	--	--
22.6	5103.71	--	--	--	--	--	--	--
23.62	4548.41	--	4485.89	--	--	4506.6	--	--
24.68	4056.12	--	4015.95	--	--	--	--	--
25.8	3612.57	--	--	--	--	--	--	--
28.03	2909.84	--	--	--	--	2862.62	--	--
31.64	2121.19	--	--	--	--	2308.26	--	--
34.17	1735.41	--	--	--	--	1844.69	--	--
36.82	1428.1	--	1446.44	--	--	--	--	--
38.18	1299.13	--	--	--	--	1320.12	--	--
41	1078.69	--	--	--	--	1088.97	--	--
43.95	899.83	--	931.91	--	--	--	--	--
45.47	823.43	--	--	--	--	796.5	--	--
46.9	759.52	--	--	--	--	--	--	--
48.6	692.13	--	686.58	--	--	--	--	--
50.2	636.03	--	611.71	--	--	--	--	--
53.54	537.63	--	--	--	--	--	501.8	--
59.5	408.2	--	--	--	--	--	--	362.44
60.62	352.42	--	--	--	--	--	319.39	--
70.27	241.34	--	--	--	--	--	223.03	--
78.71	180.41	--	--	--	--	--	175.23	--

$_{57}$La							
41.01	3190.3	--	--	--	--	3227.49	--
45.47	2436.91	--	--	--	--	2307.69	--
46.9	2247.75	--	--	--	--	--	--
53.54	1591.08	--	--	--	--	1615.13	--
59.5	1208.04	--	--	--	--	--	1239.12
60.62	1108.91	--	--	--	--	1199.67	--
70.27	759.39	--	--	--	--	772.86	--
78.71	567.68	--	--	--	--	558.3	--

Table 3. Comparaison of empirical K_β X-ray fluorescence cross-section (in barn) deduced from this work by photon impact with the experimental values of [32-38].

E(KeV)	Our results	Other Experimenrales works						
	Empirical values	Baydaş *et al.* [32]	Rao *et al*. [34]	Singh *et al.* [33]	Demir and Şahin [35]	Seven [37]	Seven and Erdoğan [36]	Özdemir *et al.* [38]
$_{28}$Ni								
8.74	1040.32	780	--	--	--	--	--	--
9.36	872.25	780	--	--	--	--	--	--
10	735.85	604	--	--	--	--	--	--
10.68	621.34	556	--	--	--	--	--	--
11.4	525.39	448	715	--	--	--	--	--
12.09	451.72	390	--	--	--	--	--	--
13.6	333.77	283	--	--	--	--	--	--
14.38	289.19	244	--	--	--	--	--	--
15.2	250.76	205	291	--	--	--	--	--
16.04	218.37	205	--	--	--	--	--	--
17.8	167.09	--	179	--	--	--	--	--
22.6	90.44	--	111	--	--	--	--	--
23.62	80.74	--	--	78	--	--	--	--
24.68	72.12	--	--	71	--	--	--	--
25.8	64.34	--	65	--	--	--	--	--
36.82	25.78	--	--	26	--	--	--	--
41	19.56	--	17	--	--	--	--	--
43.95	16.36	--	--	18	--	--	--	--
46.9	13.84	--	10	--	--	--	--	--
59.5	7.51	--	--	--	7.51	--	--	--
$_{42}$Mo								
21.57	1012.53	--	--	--	--	1035.77	--	--
22.6	898.09	--	--	--	--	--	--	--
23.62	801.73	--	872.96	--	--	796.02	--	--
24.68	716.16	--	782.16	--	--	--	--	--
25.8	638.93	--	--	--	--	--	--	--
28.03	516.28	--	--	--	--	560.42	--	--
31.64	378.11	--	--	--	--	337.08	--	--
34.17	310.26	--	--	--	--	318.44	--	--
36.82	256.05	--	285.15	--	--	--	--	--
38.18	233.25	--	--	--	--	235.29	--	--
41	194.2	--	--	--	--	178.26	--	--
43.95	162.43	--	186.38	--	--	--	--	--
45.47	148.83	--	--	--	--	140.5	--	--
46.9	137.44	--	--	--	--	--	--	--
48.6	125.42	--	141.18	--	--	--	--	--
50.2	115.4	--	125.85	--	--	--	--	--
53.54	97.79	--	--	--	--	--	79.33	--
59.5	74.55	--	--	--	--	--	--	70.52
60.62	60.38	--	--	--	--	--	63.88	--

70.27	42.07	--	--	--	--	--	38.07	--
78.71	31.88	--	--	--	--	--	27.08	--
$_{57}$La								
41.01	810.47	--	--	--	--		786.46	--
45.47	621.53	--	--	--	--		537.53	--
53.54	408.35	--	--	--	--		369.12	--
59.5	311.3	--	--	--	--		--	319.98
60.62	250.19	--	--	--	--		276.84	--
70.27	174.33	--	--	--	--		159.18	--
78.71	132.18	--	--	--	--		127.81	--

Table 4. Comparaison of empirical K_{tot} X-ray fluorescence cross-section (in barn) deduced from this work by photon impact with the experimental values of [32-38].

E(KeV)	**Our results**	**Other Experimenrales works**						
	Empirical values	Baydaş *et al.* [32]	Rao *et al*. [34]	Singh *et al.* [33]	Demir and Şahin [35]	Seven [37]	Seven and Erdoğan [36]	Özdemir *et al.* [38]
$_{28}$Ni								
8.74	10149.07	9162	--	--	--	--	--	--
9.36	8479.9	8479	--	--	--	--	--	--
10	7129.89	6939	--	--	--	--	--	--
10.68	6000.33	6501	--	--	--	--	--	--
11.4	5056.98	5126	5610	--	--	--	--	--
12.09	4334.91	4386	--	--	--	--	--	--
13.6	3184.01	3207	--	--	--	--	--	--
14.38	2750.9	2778	--	--	--	--	--	--
15.2	2378.65	2447	2428	--	--	--	--	--
16.04	2065.78	2349	--	--	--	--	--	--
17.8	1572.31	--	1506	--	--	--	--	--
22.6	840.8	--	898	--	--	--	--	--
23.62	748.91	--	--	616	--	--	--	--
24.68	667.49	--	--	567	--	--	--	--
25.8	594.17	--	540	--	--	--	--	--
32.86	315.14	--	--	--	--	--	--	--
36.82	233.85	--	--	199	--	--	--	--
41	176.4	--	139	--	--	--	--	--
43.95	147.03	--	--	134	--	--	--	--
46.9	124	--	88	--	--	--	--	--
59.5	66.45	--	--	--	53.86	--	--	--
$_{42}$Mo								
21.57	7013.72	--	--	--	--	6765.79	--	--
22.6	6206.35	--	--	--	--	6037.47	--	--
23.62	5528.06	--	5358.85	--	--	5302.62	--	--
24.68	4927.06	--	4783.78	--	--	--	--	--
25.8	4385.86	--	--	--	--	--	--	--
28.03	3529.09	--	--	--	--	3423.04	--	--
31.64	2568.75	--	--	--	--	2645.34	--	--
34.17	2099.58	--	--	--	--	2163.13	--	--
36.82	1726.18	--	1731.59	--	--	--	--	--
38.18	1569.59	--	--	--	--	1555.41	--	--
41	1302.11	--	--	--	--	1267.23	--	--
43.95	1085.27	--	1118.29	--	--	--	--	--
45.47	992.71	--	--	--	--	937	--	--
46.9	915.31	--	--	--	--	--	--	--
48.6	833.73	--	828.36	--	--	--	--	--
50.2	765.85	--	737.56	--	--	--	--	--

53.54	646.84	--	--	--	--	--	581.13	--
59.5	490.48	--	--	--	--	--	--	431.72
60.62	404.36	--	--	--	--	--	383.28	--
70.27	277.31	--	--	--	--	--	261.09	--
78.71	207.58	--	--	--	--	--	202.31	--

$_{57}$La								
41.01	4125.01	--	--	--	--		4013.95	--
45.47	3146.86	--	--	--	--		2845.22	--
53.54	2050.47	--	--	--	--		1984.25	--
59.5	1554.81	--	--	--	--		--	1558.83
60.62	1365.95	--	--	--	--		1476.48	--
70.27	936.77	--	--	--	--		932.03	--
78.71	701.23	--	--	--	--		686.10	--